应用数学和力学编委会编
重 庆 出 版 社 出 版

文章编号: 1000_0887(2001) 03_0228_11
创刊廿周年纪念特刊论文

湿热环境中复合材料层合圆柱薄壳的屈曲和后屈曲*

沈惠申

(上海交通大学 建筑工程和力学学院, 上海 200030)

(我刊编委沈惠申来稿)

摘要: 在宏_细观力学模型框架下, 讨论湿热环境对复合材料层合圆柱薄壳在轴向压缩作用下屈曲和后屈曲行为的影响• 基于细观力学模型复合材料性能与湿度和温度变化有关• 壳体控制方程基于经典层合壳理论, 并包括湿热效应• 壳体屈曲的边界层理论被推广用于湿热环境的情况, 相应的奇异摄动法用于确定层合圆柱薄壳的屈曲荷载和后屈曲平衡路径• 分析中同时计及壳体非线性前屈曲变形和初始几何缺陷的影响• 数值算例给出完善和非完善正交铺设层合圆柱薄壳在不同湿热环境中的后屈曲行为• 讨论了温度和湿度, 纤维体积比率, 壳体几何参数, 铺层数, 铺层方式和初始几何缺陷等各种参数变化的影响•

关 键 词: 结构稳定性; 后屈曲; 湿热环境; 层合圆柱壳; 壳体屈曲的边界层理论; 奇异摄动法

中图分类号: O343 文献标识码: A

引 言

纤维增强复合材料壳结构已广泛用于航空, 造船, 汽车及其他工业部门• 在结构的服役期间, 温度和湿度的变化会减小材料的弹性模量, 降低材料的强度• 因此, 需要仔细评估湿热环境对结构的不利影响•

采用经典层合壳理论讨论复合材料层合圆柱薄壳在机械荷载、热荷载或复合荷载共同作用下后屈曲行为的论文已有许多, 如文献[1~ 6]• 在所有这些研究中材料性能都假定与温度变化无关• 另一方面, 讨论湿热环境对复合材料层合平板和柱形曲板屈曲荷载的影响的论文相当有限[7~ 11], 并仅限于讨论完善结构• 事实上, 在许多情况下壳体承受高水平压应力其荷载_挠度关系是非线性的, 且此类壳结构不可避免地存在初始几何缺陷• 据作者所知, 尚无公开发表的文献讨论过复合材料层合圆柱壳在湿热环境中的后屈曲行为•

在本文研究中, 假定温度和温度的分布是均匀的, 温度和湿度的变化假定与时间和位置无关• 壳体材料性能假定是温度和湿度的函数• 材料热膨胀和吸湿膨胀系数由细观复合材料力学给出(参见 Tsai 和 Hahn[12])• 就宏观而言, 壳体控制方程基于经典层合壳理论, 并包括湿热

* 收稿日期: 1999_09_11; 修订日期: 2000_08_29
基金项目: 国家自然科学基金资助项目(59975058)
作者简介: 沈惠申(1947—), 浙江人, 男, 教授, 博士, 博导.

效应• 将壳体屈曲的边界层理论推广用于湿热环境的情况,相应的奇异摄动方法用于确定层合圆柱薄壳的屈曲荷载和后屈曲平衡路径• 分析中同时计及壳体非线性前屈曲变形和初始几何缺陷的影响• 初始缺陷的形式取作和壳体初始屈曲模态一致•

1 基本方程

考虑半径为 R,长度为 L,厚度为 t 的层合圆柱薄壳,铺层数为 N• 处于湿度和温度变化的环境中,并承受轴向压缩荷载 P 作用• 假定 U, V 和 W 为对应右手坐标系 (X, Y, Z) 的位移分量,其中 X、Y 和 Z 分别为壳体中面轴各、周向和法向(向内指向为正)坐标• 以 $W^*(X, Y)$ 和 $W(X, Y)$ 分别表示圆柱壳的初始的和附加的挠度,以 $F(X, Y)$ 表示应力函数,并以逗号表示微分求导,那么 $N_x = F_{,yy}$, $N_y = F_{,xx}$ 和 $N_{xy} = -F_{,xy}$•

考虑正交铺设层合圆柱薄壳,由经典层合壳理论(即忽略横向剪切变形的影响)并计及湿热效应,其控制方程为

$$L_{11}(W) + L_{12}(F) - L_{13}(N^H) - L_{14}(M^H) - \frac{1}{R}F_{,xx} = L(W + W^*, F), \tag{1}$$

$$L_{21}(F) - L_{22}(W) - L_{23}(N^H) + \frac{1}{R}W_{,xx} = -\frac{1}{2}L(W + 2W^*, W), \tag{2}$$

其中算子

$$\begin{cases} L_{11}(\ ) = D^*_{11}\dfrac{\partial^4}{\partial X^4} + 2(D^*_{12} + 2D^*_{66})\dfrac{\partial^4}{\partial X^2\partial Y^2} + D^*_{22}\dfrac{\partial^4}{\partial Y^4}, \\ L_{12}(\ ) = L_{22}(\ ) = B^*_{21}\dfrac{\partial^4}{\partial X^4} + (B^*_{11} + B^*_{22} - 2B^*_{66})\dfrac{\partial^4}{\partial X^2\partial Y^2} + B^*_{12}\dfrac{\partial^4}{\partial Y^4}, \\ L_{13}(N^H) = \dfrac{\partial^2}{\partial X^2}(B^*_{11}N^H_x + B^*_{21}N^H_y) + 2\dfrac{\partial^2}{\partial X\partial Y}(B^*_{66}N^H_{xy}) + \dfrac{\partial^2}{\partial Y^2}(B^*_{12}N^H_x + B^*_{22}N^H_y), \\ L_{14}(M^H) = \dfrac{\partial^2}{\partial X^2}(M^H_x) + 2\dfrac{\partial^2}{\partial X\partial Y}(M^H_{xy}) + \dfrac{\partial^2}{\partial Y^2}(M^H_y), \\ L_{21}(\ ) = A^*_{22}\dfrac{\partial^4}{\partial X^4} + (2A^*_{12} + A^*_{66})\dfrac{\partial^4}{\partial X^2\partial Y^2} + A^*_{11}\dfrac{\partial^4}{\partial Y^4}, \\ L_{23}(N^H) = \dfrac{\partial^2}{\partial X^2}(A^*_{12}N^H_x + A^*_{22}N^H_y) - \dfrac{\partial^2}{\partial X\partial Y}(A^*_{66}N^H_{xy}) + \dfrac{\partial^2}{\partial Y^2}(A^*_{11}N^H_x + A^*_{12}N^H_y), \\ L(\ ) = \dfrac{\partial^2}{\partial X^2}\dfrac{\partial^2}{\partial Y^2} - 2\dfrac{\partial^2}{\partial X\partial Y}\dfrac{\partial^2}{\partial X\partial Y} + \dfrac{\partial^2}{\partial Y^2}\dfrac{\partial^2}{\partial X^2}• \end{cases} \tag{3}$$

壳体平均端部轴向缩短量为

$$\begin{aligned} \frac{\Delta_x}{L} &= -\frac{1}{2\pi RL}\int_0^{2\pi R}\int_0^L \frac{\partial U}{\partial X}\mathrm{d}X\,\mathrm{d}Y = \\ &-\frac{1}{2\pi RL}\int_0^{2\pi R}\int_0^L\Bigg[A^*_{11}\frac{\partial^2 F}{\partial Y^2} + A^*_{12}\frac{\partial^2 F}{\partial X^2} - \left(B^*_{11}\frac{\partial^2 W}{\partial X^2} + B^*_{12}\frac{\partial^2 W}{\partial Y^2}\right) - \\ &\frac{1}{2}\left(\frac{\partial W}{\partial X}\right)^2 - \frac{\partial W}{\partial X}\frac{\partial W^*}{\partial X} - (A^*_{11}N^H_x + A^*_{12}N^H_y)\Bigg]\mathrm{d}X\,\mathrm{d}Y, \end{aligned} \tag{4}$$

闭合条件(或周期性条件)为

$$\int_0^{2\pi R}\frac{\partial V}{\partial Y}\mathrm{d}Y = 0, \tag{5a}$$

即

$$\int_0^{2\pi R}\left[A_{22}^*\frac{\partial^2 F}{\partial X^2}+A_{12}^*\frac{\partial^2 F}{\partial Y^2}-\left(B_{21}^*\frac{\partial^2 W}{\partial X^2}+B_{22}^*\frac{\partial^2 W}{\partial Y^2}\right)+\frac{W}{R}-\frac{1}{2}\left(\frac{\partial W}{\partial Y}\right)^2-\frac{\partial W}{\partial Y}\frac{\partial W^*}{\partial Y}-(A_{12}^*N_x^{\mathrm{H}}+A_{22}^*N_y^{\mathrm{H}})\right]\mathrm{d}Y=0, \tag{5b}$$

壳体端部边界假定为简支或固支的,那么边界条件为

沿 $X=0, L$ 边界

$$W=0,\ M_x=-B_{11}^*\frac{\partial^2 F}{\partial X^2}-B_{12}^*\frac{\partial^2 F}{\partial Y^2}-D_{11}^*\frac{\partial^2 W}{\partial X^2}-D_{12}^*\frac{\partial^2 W}{\partial Y^2}+M^{\mathrm{H}}=0\quad(\text{简支}), \tag{6a}$$

$$W=W_{,x}=0\quad(\text{固支}), \tag{6b}$$

$$\int_0^{2\pi R}N_x\,\mathrm{d}Y+2\pi Rt\sigma_x=0, \tag{6c}$$

其中 σ_x 为平均轴向压应力, M_x 为单位长度上的弯矩•

湿热荷载定义为

$$\begin{bmatrix}N^{\mathrm{H}}\\ M^{\mathrm{H}}\end{bmatrix}=\begin{bmatrix}N^{\mathrm{T}}\\ M^{\mathrm{T}}\end{bmatrix}+\begin{bmatrix}N^{\mathrm{m}}\\ M^{\mathrm{m}}\end{bmatrix}, \tag{7}$$

由温度或湿度增量引起的内力和弯矩为

$$\begin{bmatrix}N_x^{\mathrm{T}} & M_x^{\mathrm{T}}\\ N_y^{\mathrm{T}} & M_y^{\mathrm{T}}\\ N_{xy}^{\mathrm{T}} & M_{xy}^{\mathrm{T}}\end{bmatrix}=\sum_{k=1}^{N}\int_{t_{k-1}}^{t_k}(1,Z)\begin{bmatrix}A_x\\ A_y\\ A_{xy}\end{bmatrix}_k\Delta T\,\mathrm{d}Z, \tag{8a}$$

或

$$\begin{bmatrix}N_x^{\mathrm{m}} & M_x^{\mathrm{m}}\\ N_y^{\mathrm{m}} & M_y^{\mathrm{m}}\\ N_{xy}^{\mathrm{m}} & M_{xy}^{\mathrm{m}}\end{bmatrix}=\sum_{k=1}^{N}\int_{t_{k-1}}^{t_k}(1,Z)\begin{bmatrix}B_x\\ B_y\\ B_{xy}\end{bmatrix}_k\Delta C\,\mathrm{d}Z, \tag{8b}$$

其中 ΔT 为相对无热应变的参考温度引起的温度增量, ΔC 为相对零湿度引起的湿度增量, 且

$$\begin{bmatrix}A_x\\ A_y\\ A_{xy}\end{bmatrix}=-\begin{bmatrix}Q_{11} & Q_{12} & Q_{16}\\ Q_{12} & Q_{22} & Q_{26}\\ Q_{16} & Q_{26} & Q_{66}\end{bmatrix}\begin{bmatrix}c^2 & s^2\\ s^2 & c^2\\ 2cs & -2cs\end{bmatrix}\begin{bmatrix}\alpha_{11}\\ \alpha_{22}\end{bmatrix}, \tag{9a}$$

$$\begin{bmatrix}B_x\\ B_y\\ B_{xy}\end{bmatrix}=-\begin{bmatrix}Q_{11} & Q_{12} & Q_{16}\\ Q_{12} & Q_{22} & Q_{26}\\ Q_{16} & Q_{26} & Q_{66}\end{bmatrix}\begin{bmatrix}c^2 & s^2\\ s^2 & c^2\\ 2cs & -2cs\end{bmatrix}\begin{bmatrix}\beta_{11}\\ \beta_{22}\end{bmatrix}, \tag{9b}$$

其中 Q_{ij} 为转换弹性常数, 定义为

$$\begin{bmatrix}Q_{11}\\ Q_{12}\\ Q_{22}\\ Q_{16}\\ Q_{26}\\ Q_{66}\end{bmatrix}=\begin{bmatrix}c^4 & 2c^2s^2 & s^4 & 4c^2s^2\\ c^2s^2 & c^4+s^4 & c^2s^2 & -4c^2s^2\\ s^4 & 2c^2s^2 & c^4 & 4c^2s^2\\ c^3s & cs^3-c^3s & -cs^3 & -2cs(c^2-s^2)\\ cs^3 & c^3s-cs^3 & -c^3s & 2cs(c^2-s^2)\\ c^2s^2 & -2c^2s^2 & c^2s^2 & (c^2-s^2)^2\end{bmatrix}\begin{bmatrix}Q_{11}\\ Q_{12}\\ Q_{22}\\ Q_{66}\end{bmatrix}, \tag{10a}$$

其中

$$Q_{11}=\frac{E_{11}}{(1-\nu_{12}\nu_{21})},\quad Q_{22}=\frac{E_{22}}{(1-\nu_{12}\nu_{21})},\quad Q_{12}=\frac{\nu_{21}E_{11}}{(1-\nu_{12}\nu_{21})},\quad Q_{66}=G_{12},\tag{10b}$$

及

$$c=\cos\theta,\quad s=\sin\theta,\tag{10c}$$

其中 θ 为相对壳体 X 轴的铺设角•

基于细观力学模型, 复合材料热膨胀系数可表为[12]

$$\alpha_{11}=\frac{V_{\rm f}E_{\rm f}\alpha_{\rm f}+V_{\rm m}E_{\rm m}\alpha_{m}}{V_{\rm f}E_{\rm f}+V_{\rm m}E_{\rm m}},\tag{11a}$$

$$\alpha_{22}=(1+\nu_{\rm f})V_{\rm f}\alpha_{\rm f}+(1+\nu_{\rm m})V_{\rm m}\alpha_{\rm m}-\nu_{12}\alpha_{11},\tag{11b}$$

其中 $\alpha_{\rm f}$ 和 $\alpha_{\rm m}$ 分别为纤维和基体的热膨胀系数, 而吸湿膨胀系数可表示为

$$\beta_{11}=\frac{V_{\rm f}E_{\rm f}c_{\rm fm}\beta_{\rm f}+V_{\rm m}E_{\rm m}\beta_{\rm m}}{E_{11}(V_{\rm f}\rho_{\rm f}c_{\rm fm}+V_{\rm m}\rho_{\rm m})}\rho,\tag{12a}$$

$$\beta_{22}=\frac{V_{\rm f}(1+\nu_{\rm f})c_{\rm fm}\beta_{\rm f}+V_{\rm m}(1+\nu_{\rm m})\beta_{\rm m}}{V_{\rm f}\rho_{\rm f}c_{\rm fm}+V_{\rm m}\rho_{\rm m}}\rho-\nu_{12}\beta_{11},\tag{12b}$$

其中 $c_{\rm fm}$ 为吸湿率; $\beta_{\rm f}$ 和 $\beta_{\rm m}$ 分别为纤维和基体的吸湿膨胀系数; ρ, $\rho_{\rm f}$ 和 $\rho_{\rm m}$ 分别为复合材料层板、纤维和基体的密度, 其相互关系为

$$\rho=V_{\rm f}\rho_{\rm f}+V_{\rm m}\rho_{\rm m}\cdot\tag{13}$$

在以上公式中 $V_{\rm f}$ 和 $V_{\rm m}$ 分别为纤维和基体的体积比率, 且有

$$V_{\rm f}+V_{\rm m}=1,\tag{14}$$

其中 $E_{\rm f}$、$G_{\rm f}$ 和 $\nu_{\rm f}$ 分别为纤维的弹性模量、剪切弹性模量和Poisson比, $E_{\rm m}$、$G_{\rm m}$ 和 $\nu_{\rm m}$ 则分别为基体的弹性模量、剪切弹性模量和Poisson 比• 那么

$$E_{11}=V_{\rm f}E_{\rm f}+V_{\rm m}E_{\rm m},\tag{15a}$$

$$\frac{1}{E_{22}}=\frac{V_{\rm f}}{E_{\rm f}}+\frac{V_{\rm m}}{E_{\rm m}}-V_{\rm f}V_{\rm m}\frac{\nu_{\rm f}^2E_{\rm m}/E_{\rm f}+\nu_{\rm m}^2E_{\rm f}/E_{\rm m}-2\nu_{\rm f}\nu_{\rm m}}{V_{\rm f}E_{\rm f}+V_{\rm m}E_{\rm m}},\tag{15b}$$

$$\frac{1}{G_{12}}=\frac{V_{\rm f}}{G_{\rm f}}+\frac{V_{\rm m}}{G_{\rm m}},\tag{15c}$$

$$\nu_{12}=V_{\rm f}\nu_{\rm f}+V_{\rm m}\nu_{\rm m},\tag{15d}$$

由于 $E_{\rm m}$ 是温度和湿度变化的函数, 因此 α_{11}、α_{22}、β_{22}、E_{11}、E_{22} 和 G_{12} 皆为温度和湿度变化的函数• 同样, “约化” 刚度矩阵 $[A^*_{ij}]$、$[B^*_{ij}]$ 和 $[D^*_{ij}]$ $(i,j=1,2,6)$ 亦为温度和湿度变化的函数, 定义为

$$\boldsymbol{A}^*=\boldsymbol{A}^{-1},\quad \boldsymbol{B}^*=-\boldsymbol{A}^{-1}\boldsymbol{B},\quad \boldsymbol{D}^*=\boldsymbol{D}-\boldsymbol{B}\boldsymbol{A}^{-1}\boldsymbol{B},\tag{16}$$

其中 A_{ij}, B_{ij} 和 D_{ij} 定义为

$$[A_{ij},B_{ij},D_{ij}]=\sum_{k=1}^{N}\int_{t_{k-1}}^{t_k}(Q_{ij})_k(1,Z,Z^2)\,\mathrm{d}Z\qquad(i,j=1,2,6)\cdot\tag{17}$$

2　分析方法与渐近解

依据上述公式我们现在来构造满足方程(1)和(2)及边界条件(6)的解• 首先引进无量纲量

$$\begin{cases} x = \pi X/L,\ y = Y/R,\ \beta = L/\pi R,\ Z = L^2/Rt,\ \varepsilon = (\pi^2 R/L^2)[D_{11}^* D_{22}^* A_{11}^* A_{22}^*]^{1/4}, \\ (W, W^*) = \varepsilon(W, W^*)/[D_{11}^* D_{22}^* A_{11}^* A_{22}^*]^{1/4},\ F = \varepsilon^2 F/[D_{11}^* D_{22}^*]^{1/2}, \\ \gamma_{12} = (D_{12}^* + 2D_{66}^*)/D_{11}^*,\ \gamma_{14} = [D_{22}^*/D_{11}^*]^{1/2},\ \gamma_{22} = (A_{12}^* + A_{66}^*/2)/A_{22}^*, \\ \gamma_{24} = [A_{11}^*/A_{22}^*]^{1/2},\ \gamma_5 = -A_{12}^*/A_{22}^*, \\ (\gamma_{30}, \gamma_{32}, \gamma_{34}, \gamma_{311}, \gamma_{322}) = (B_{21}^*, B_{11}^* + B_{22}^* - 2B_{66}^*, B_{12}^*, B_{11}^*, B_{22}^*)/[D_{11}^* D_{22}^* A_{11}^* A_{22}^*]^{1/4}, \\ (\gamma_{T1}, \gamma_{T2}, \gamma_{T3}, \gamma_{T4}) = (A_x^T, A_y^T, B_x^m, B_y^m) R/[D_{11}^* D_{22}^*/A_{11}^* A_{22}^*]^{1/4}, \\ M_x = \varepsilon^2 M_x L^2/\pi^2 D_{11}^* [D_{11}^* D_{22}^* A_{11}^* A_{22}^*]^{1/4}, \\ \lambda_p = \sigma_x/(2/Rt)[D_{11}^* D_{22}^*/A_{11}^* A_{22}^*]^{1/4},\ \delta_x = (\Delta_x/L)/(2/R)[D_{11}^* D_{22}^* A_{11}^* A_{22}^*]^{1/4}, \end{cases} \tag{18}$$

及

$$\begin{bmatrix} A_x^T & B_x^m \\ A_y^T & B_y^m \end{bmatrix} = -\sum_{k=1}^{N} \int_{t_{k-1}}^{t_k} \begin{bmatrix} A_x & B_x \\ A_y & B_y \end{bmatrix}_k \mathrm{d}Z, \tag{19}$$

那么,非线性方程(1)和(2)可表为如下无量纲形式

$$\varepsilon^2 L_{11}(W) + \varepsilon\gamma_{14} L_{12}(F) - \gamma_{14} F_{,xx} = \gamma_{14}\beta^2 L(W + W^*, F), \tag{20}$$

$$L_{21}(F) - \varepsilon\gamma_{24} L_{22}(W) + \gamma_{24} W_{,xx} = -\frac{1}{2}\gamma_{24}\beta^2 L(W + 2W^*, W), \tag{21}$$

其中

$$\begin{cases} L_{11}(\ ) = \dfrac{\partial^4}{\partial x^4} + 2\gamma_{12}\beta^2 \dfrac{\partial^4}{\partial x^2 \partial y^2} + \gamma_{14}^2 \beta^4 \dfrac{\partial^4}{\partial y^4}, \\ L_{12}(\ ) = L_{22}(\ ) = \gamma_{30} \dfrac{\partial^4}{\partial x^4} + \gamma_{32}\beta^2 \dfrac{\partial^4}{\partial x^2 \partial y^2} + \gamma_{34}\beta^4 \dfrac{\partial^4}{\partial y^4}, \\ L_{21}(\ ) = \dfrac{\partial^4}{\partial x^4} + 2\gamma_{22}\beta^2 \dfrac{\partial^4}{\partial x^2 \partial y^2} + \gamma_{24}^2 \beta^4 \dfrac{\partial^4}{\partial y^4}, \\ L(\ ) = \dfrac{\partial^2}{\partial x^2}\dfrac{\partial^2}{\partial y^2} - 2\dfrac{\partial^2}{\partial x \partial y}\dfrac{\partial^2}{\partial x \partial y} + \dfrac{\partial^2}{\partial y^2}\dfrac{\partial^2}{\partial x^2}. \end{cases} \tag{22}$$

由于湿度和温度增量 ΔC 和 ΔT 与坐标无关,因此方程(1)和(2)中的湿热耦合算子消失,但下式(23)和(24)中仍含有 ΔC 和 ΔT.

壳体端部轴向缩短量化为

$$\delta_x = -\frac{1}{4\pi^2\gamma_{24}}\varepsilon^{-1}\int_0^{2\pi}\int_0^{\pi}\left[\gamma_{24}^2\beta^2\frac{\partial^2 F}{\partial y^2} - \gamma_5\frac{\partial^2 F}{\partial x^2} - \varepsilon\gamma_{24}\left(\gamma_{311}\frac{\partial^2 W}{\partial x^2} + \gamma_{34}\beta^2\frac{\partial^2 W}{\partial y^2}\right) - \frac{1}{2}\gamma_{24}\left(\frac{\partial W}{\partial x}\right)^2 - \gamma_{24}\frac{\partial W}{\partial x}\frac{\partial W^*}{\partial x} + (\gamma_{24}^2\gamma_{T1} - \gamma_5\gamma_{T2})\Delta T + (\gamma_{24}^2\gamma_{T3} - \gamma_5\gamma_{T4})\Delta C\right]\mathrm{d}x\,\mathrm{d}y; \tag{23}$$

闭合条件化为

$$\int_0^{2\pi}\left[\left(\frac{\partial^2 F}{\partial x^2} - \gamma_5\beta^2\frac{\partial^2 F}{\partial y^2}\right) - \varepsilon\gamma_{24}\left(\gamma_{30}\frac{\partial^2 W}{\partial x^2} + \gamma_{322}\beta^2\frac{\partial^2 W}{\partial y^2}\right) + \gamma_{24}W - \frac{1}{2}\gamma_{24}\beta^2\left(\frac{\partial W}{\partial y}\right)^2 - \gamma_{24}\beta^2\frac{\partial W}{\partial y}\frac{\partial W^*}{\partial y} + (\gamma_{T2} - \gamma_5\gamma_{T1})\Delta T + (\gamma_{T4} - \gamma_5\gamma_{T3})\Delta C\right]\mathrm{d}y = 0; \tag{24}$$

边界条件式(6)化为

$x = 0, \pi$:

$$W = M_x = 0 \quad (简支), \tag{25a}$$

$$W = W_{,x} = 0 \quad (固支), \tag{25b}$$

$$\frac{1}{2\pi}\int_0^{2\pi} \beta^2 \frac{\partial^2 F}{\partial y^2}\mathrm{d}y + 2\lambda_p \varepsilon^2 = 0. \tag{25c}$$

对于各向同性圆柱壳，由式(18)我们有 $\varepsilon = \pi^2/Z_B\sqrt{12}$，其中 $Z_B = (L^2/Rt)[1-\nu^2]^{1/2}$ 为 Batdorf 壳体几何参数，对于经典圆柱壳屈曲问题其值应大于2.85(参见Batdorf[13])。当 $Z_B >$ 2.85时导出 $\varepsilon < 1$，方程(20)和(21)即为边界层型方程。此方程可同时考虑壳体非线性前屈曲变形、后屈曲大挠度和初始几何缺陷的影响。

依据式(20)~(25)，采用奇异摄动方法可确定完善和非完善，层合圆柱薄壳在不同湿热环境条件下的后屈曲行为。假定方程(20)和(21)的解为

$$\begin{aligned} W &= w(x, y, \varepsilon) + \widetilde{W}(x, \xi, y, \varepsilon) + \widehat{W}(x, \zeta, y, \varepsilon), \\ F &= f(x, y, \varepsilon) + \widetilde{F}(x, \xi, y, \varepsilon) + \widehat{W}(x, \zeta, y, \varepsilon), \end{aligned} \tag{26}$$

其中 ε 为摄动小参数，如式(18)所定义。$w(x, y, \varepsilon)$、$f(x, y, \varepsilon)$ 称为壳体的“外解”或正则解，$\widetilde{W}(x, \xi, y, \varepsilon)$、$\widetilde{F}(x, \xi, y, \varepsilon)$ 和 $\widehat{W}(x, \zeta, y, \varepsilon)$、$\widehat{F}(x, \zeta, y, \varepsilon)$ 分别为 $x = 0$ 和 $x = \pi$ 端的边界层解，且边界层变量 ξ 和 ζ 定义为

$$\xi = x/\sqrt{\varepsilon}, \qquad \zeta = (\pi - x)/\sqrt{\varepsilon} \tag{27}$$

(这意味着对于各向同性圆柱壳，边界层宽度为 $\sqrt{Rt}$ 量级)。将式(26)中的正则解和边界层解展为如下渐近展开式

$$w(x, y, \varepsilon) = \sum_{j=1} \varepsilon^j w_j(x, y), \quad f(x, y, \varepsilon) = \sum_{j=0} \varepsilon^j f_j(x, y), \tag{28a}$$

$$\widetilde{W}(x, \xi, y, \varepsilon) = \sum_{j=0} \varepsilon^{j+1} \widetilde{W}_{j+1}(x, \xi, y), \quad \widetilde{F}(x, \zeta, y, \varepsilon) = \sum_{j=0} \varepsilon^{j+2} \widetilde{F}_{j+2}(x, \xi, y), \tag{28b}$$

$$\widehat{W}(x, \zeta, y, \varepsilon) = \sum_{j=0} \varepsilon^{j+1} \widehat{W}_{j+1}(x, \zeta, y), \quad \widehat{F}(x, \zeta, y, \varepsilon) = \sum_{j=0} \varepsilon^{j+2} \widehat{F}_{j+2}(x, \zeta, y). \tag{28c}$$

壳体初始屈曲模态假定为

$$w_2(x, y) = A_{11}^{(2)} \sin mx \sin ny. \tag{29}$$

壳体初始几何缺陷假定具有相同的形式，即

$$W^*(x, y, \varepsilon) = \varepsilon^2 a_{11}^* \sin mx \sin ny = \varepsilon^2 \mu A_{11}^{(2)} \sin mx \sin ny, \tag{30}$$

其中 $\mu = a_{11}^*/A_{11}^{(2)}$ 为缺陷参数。

将式(26)~(28)代入方程方程(20)和(21)，可得正则解和边界层解各自应满足的三组摄动方程，利用式(29)和(30)逐级求解这些摄动方程组，并在壳体两端匹配正则解和边界层解，可以导得满足固支边界条件的大挠度渐近解

$$\begin{aligned} W = {} & \varepsilon\Bigg[A_{00}^{(1)} - A_{00}^{(1)}\left(\cos\phi\frac{x}{\sqrt{\varepsilon}} + \frac{\alpha}{\phi}\sin\phi\frac{x}{\sqrt{\varepsilon}}\right)\exp\left(-\alpha\frac{x}{\sqrt{\varepsilon}}\right) - \\ & A_{00}^{(1)}\left(\cos\phi\frac{\pi - x}{\sqrt{\varepsilon}} + \frac{\alpha}{\phi}\sin\phi\frac{\pi - x}{\sqrt{\varepsilon}}\right)\exp\left(-\alpha\frac{\pi - x}{\sqrt{\varepsilon}}\right)\Bigg] + \\ & \varepsilon^2\Bigg[A_{11}^{(2)} \sin mx \sin ny + A_{02}^{(2)} \cos 2ny - \\ & A_{02}^{(2)} \cos 2ny\left(\cos\phi\frac{x}{\sqrt{\varepsilon}} + \frac{\alpha}{\phi}\sin\phi\frac{x}{\sqrt{\varepsilon}}\right)\exp\left(-\alpha\frac{x}{\sqrt{\varepsilon}}\right) - \\ & A_{02}^{(2)} \cos 2ny\left(\cos\phi\frac{\pi - x}{\sqrt{\varepsilon}} + \frac{\alpha}{\phi}\sin\phi\frac{\pi - x}{\sqrt{\varepsilon}}\right)\exp\left(-\alpha\frac{\pi - x}{\sqrt{\varepsilon}}\right)\Bigg] + \end{aligned}$$

$$\varepsilon^3[A_{11}^{(3)}\sin mx\sin ny + A_{02}^{(3)}\cos 2ny] + \varepsilon^4[A_{00}^{(4)} + A_{20}^{(4)}\sin 2mx + A_{02}^{(4)}\cos 2ny + A_{13}^{(4)}\sin mx\sin 3ny + A_{04}^{(4)}\cos 4ny] + O(\varepsilon^5), \tag{31}$$

$$\begin{aligned}F = &-B_{00}^{(0)}\frac{y^2}{2} + \varepsilon\left[-B_{00}^{(1)}\frac{y^2}{2}\right] + \varepsilon^2\Bigg[-B_{00}^{(2)}\frac{y^2}{2} + B_{11}^{(2)}\sin mx\sin ny + \\ &A_{00}^{(1)}\left\{\gamma_{24}\left(\frac{1}{b}+\gamma_{30}\right)\cos\phi\frac{x}{\sqrt{\varepsilon}} - \gamma_{24}\left(\frac{1}{b}-\gamma_{30}\right)\frac{\alpha}{\phi}\sin\phi\frac{x}{\sqrt{\varepsilon}}\right\}\exp\left(-\alpha\frac{x}{\sqrt{\varepsilon}}\right) + \\ &A_{00}^{(1)}\left\{\gamma_{24}\left(\frac{1}{b}+\gamma_{30}\right)\cos\phi\frac{\pi-x}{\sqrt{\varepsilon}} - \gamma_{24}\left(\frac{1}{b}-\gamma_{30}\right)\frac{\alpha}{\phi}\sin\phi\frac{\pi-x}{\sqrt{\varepsilon}}\right\}\times \\ &\exp\left(-\alpha\frac{\pi-x}{\sqrt{\varepsilon}}\right)\Bigg] + \varepsilon^3\Bigg[-B_{00}^{(3)}\frac{y^2}{2} + B_{02}^{(3)}\cos 2ny + \\ &A_{02}^{(2)}\cos 2ny\left\{\gamma_{24}\left(\frac{1}{b}+\gamma_{30}\right)\cos\phi\frac{x}{\sqrt{\varepsilon}} - \gamma_{24}\left(\frac{1}{b}-\gamma_{30}\right)\frac{\alpha}{\phi}\sin\phi\frac{x}{\sqrt{\varepsilon}}\right\}\exp\left(-\alpha\frac{x}{\sqrt{\varepsilon}}\right) + \\ &A_{02}^{(2)}\cos 2ny\left\{\gamma_{24}\left(\frac{1}{b}+\gamma_{30}\right)\cos\phi\frac{\pi-x}{\sqrt{\varepsilon}} - \gamma_{24}\left(\frac{1}{b}-\gamma_{30}\right)\frac{\alpha}{\phi}\sin\phi\frac{\pi-x}{\sqrt{\varepsilon}}\right\}\exp\left(-\alpha\frac{\pi-x}{\sqrt{\varepsilon}}\right)\Bigg] + \\ &\varepsilon^4\Bigg[-B_{00}^{(4)}\frac{y^2}{2} + B_{11}^{(4)}\sin mx\sin ny + B_{20}^{(4)}\cos 2mx + B_{02}^{(4)}\cos 2ny + \\ &B_{13}^{(4)}\sin mx\sin 3ny\Bigg] + O(\varepsilon^5). \end{aligned} \tag{32}$$

式(31)和(32)中各系数相互联系，皆可表为 $A_{11}^{(2)}$ 的函数，为简洁起见，具体表达式不再给出.

进一步，将式(31)和(32)代入边界条件(25c)，闭合条件(24)和式(23)，我们可以导得后屈曲平衡路径

$$\lambda_p = \lambda_p^{(0)} + \lambda_p^{(2)}(A_{11}^{(2)}\varepsilon)^2 + \lambda_p^{(4)}(A_{11}^{(2)}\varepsilon)^4 + \cdots \tag{33}$$

和

$$\delta_x = \delta_p^{(0)} - \delta_{\mathrm{H}}^{(0)} + \delta_p^{(2)}(A_{11}^{(2)}\varepsilon)^2 + \delta_p^{(4)}(A_{11}^{(2)}\varepsilon)^4 + \cdots \tag{34}$$

式(33)和(34)中，$(A_{11}^{(2)}\varepsilon)$ 可视为二次摄动参数，其值与壳体最大无量纲挠度有关，即

$$A_{11}^{(2)}\varepsilon = W_{\mathrm{m}} - \Theta_1 W_{\mathrm{m}}^2 + \cdots, \tag{35}$$

其中 W_{m} 为壳体最大无量纲挠度，假定取在$(x, y) = (\pi/2m, \pi/2n)$ 点，且

$$W_{\mathrm{m}} = \frac{1}{C_3}\left[\frac{1}{[D_{11}^*D_{22}^*A_{11}^*A_{22}^*]^{1/4}}\frac{W}{t} + \Theta_2\right]. \tag{36}$$

在式(34)和(36)中

$$\delta_{\mathrm{H}}^{(0)} = \frac{1}{2\gamma_{24}}[(\gamma_{24}^2\gamma_{T1} - \gamma_5\gamma_{T2})\Delta T + (\gamma_{24}^2\gamma_{T3} - \gamma_5\gamma_{T4})\Delta C], \tag{37a}$$

$$\Theta_2 = \frac{1}{\gamma_{24}}[(\gamma_{T2} - \gamma_5\gamma_{T1})\Delta T + (\gamma_{T4} - \gamma_5\gamma_{T3})\Delta C] + 2\frac{\gamma_5}{\gamma_{24}}\lambda_p^{(0)}. \tag{37b}$$

式(33)～(37)中所有其它符号如文献[4]所定义. 需要指出，现在 $\lambda_p^{(i)}$ 和 $\delta_p^{(i)}(i = 0, 2, 4)$ 皆为温度和湿度变化的函数.

式(33)和(34)可用于复合材料层合圆柱壳在不同湿热环境条件下的后屈曲荷载_缩短曲线(或荷载_挠度曲线)计算. 由于忽略了横向剪切变形效应的影响，壳体的径厚比的取值应大于50，面内弹性模量比的取值应小于25，即 $R/t > 50$ 和 $E_{11}/E_{22} < 25$. 对于完善壳体取 $W^*/t = 0$(或 $\mu = 0$)，并取 $W/t = 0$(注意 $W_{\mathrm{m}} \neq 0$)，我们容易求得屈曲荷载，其相应的屈曲模态为(m, n)，分别对应 X_方向的半波数和 Y_方向的全波数. 由式(31)可以看出，由于边界层解的贡献，壳体前屈曲变形是非线性的. 因此，本文得到的屈曲荷载与小挠度经典解是不同的.

3　算例和讨论

为研究温度和湿度变化对复合材料层合圆柱壳后屈曲行为的影响,给出多种完善和非完善正交铺设层合圆柱薄壳在不同湿热环境条件下的数值算例。算例选用石墨/环氧复合材料,但本文分析方法对其他复合材料同样适用。对于所有算例取 $R/t=100$, 壳板厚度 $t=0.5$ cm, 且各单层且有相同的厚度, 材料性能常数为[12, 14, 15]: $E_f=230.0$ GPa, $G_f=9.0$ GPa, $\nu_f=0.203$, $\alpha_f=-0.54\times10^{-6}$/℃, $\rho_f=1750$ kg/m^3 $=1.75$ g/cm^2, $c_{fm}=0$, $\nu_m=0.34$, $\alpha_m=45.0\times10^{-6}$/℃, $\rho_m=1200$ kg/m^3 $=1.2$ g/cm^2, $\beta_m=2.68\times10^{-3}$/wt% H_2O 和 $E_m=(3.51\times0.003T-0.142C)$ GPa, 其中 $T=T_0+\Delta T$, 且 $T_0=25$℃(室温), 及 $C=C_0+\Delta C$, 且 $C_0=0$wt% H_2O。

表1　$(0/90)_s$ 和 $(0/90)_{2T}$ 正交铺设层合圆柱壳 $(Z=500)$ 在三种湿热环境条件下的轴压屈曲应力 σ_{cr}(N/mm^2) 比较

	$(0/90)_s$			$(0/90)_{2T}$		
湿热环境条件	$V_f=0.5$	$V_f=0.6$	$V_f=0.7$	$V_f=0.5$	$V_f=0.6$	$V_f=0.7$
$\Delta T=0$℃, $\Delta C=0$%	85.716	101.872	122.595	91.429	108.556	130.007
$\Delta T=50$℃, $\Delta C=0.5$%	83.623	99.540	119.905	89.369	106.240	127.410
$\Delta T=100$℃, $\Delta C=1$%	81.493	97.087	117.150	87.271	103.873	124.744

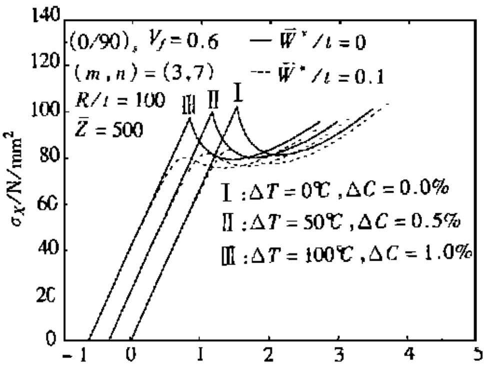

图1　湿热环境对 $(0/90)_s$ 层合圆柱壳后屈曲行为的影响

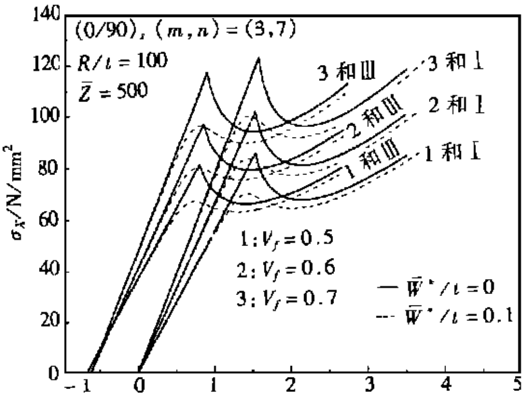

图2　在湿热环境下,纤维体积比率对 $(0/90)_s$ 层合圆柱壳后屈曲行为的影响

我们计算了 $(0/90)_s$ 和 $(0/90)_{2T}$ 正交铺设层合圆柱壳 $(Z=500)$ 在三种湿热环境条件下的屈曲应力,计算结果列在表1中。三种湿热环境条件分别记Ⅰ,Ⅱ和Ⅲ。对于情况Ⅰ, $T=25$℃, 因此 ΔT 和 ΔC 皆为零。对于情况Ⅱ, $T=75$℃, $\Delta C=0.5$%; 对于情况Ⅲ, $T=125$℃, $\Delta C=1.0$%。

图1~6为参数分析的主要结果。所有图中 W^*/t 和 W/t 分别表示壳体无量纲最大初始几何缺陷和附加挠度。

图1给出完善 $(W^*/t=0)$ 和非完善 $(W^*/t=0.1)$, $(0/90)_s$ 对称正交铺设层合圆柱壳 $(Z$

= 500和 V_f = 0.6) 在三种湿热环境条件(Ⅰ ~ Ⅲ) 下的后屈曲荷载 _缩短曲线• 由图1可见熟知的"跳跃" 式后屈曲平衡路径, 据此可计算壳体的缺陷敏感度• 图示表明, 温度和湿度的增加将降低屈曲荷载, 并使后屈曲平衡路径变得稍低•

图2给出纤维体积比率 V_f(= 0.5, 0.6和0.7) 对(0/90)s 正交铺设层合圆柱壳后屈曲行为的影响, 湿热环境条件对应Ⅰ 和 Ⅲ• 图示表明, 纤维体积比率愈高, 屈曲和后屈曲强度降低愈多•

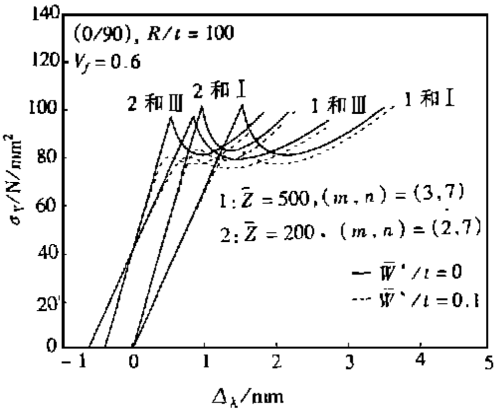

图3 在湿热环境下, 壳体几何参数对(0/90)s 层合圆柱壳后屈曲行为的影响

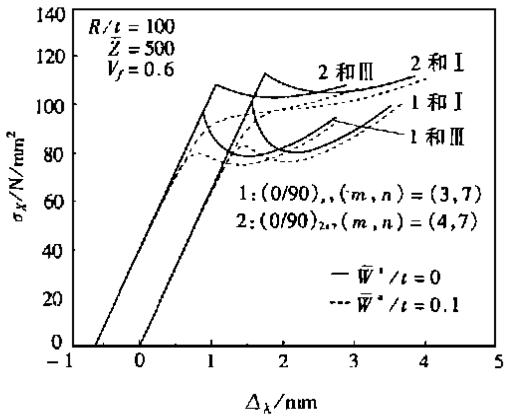

图4 在湿热环境下, 不同铺层数 N 对正交铺设层合圆柱壳后屈曲行为的影响

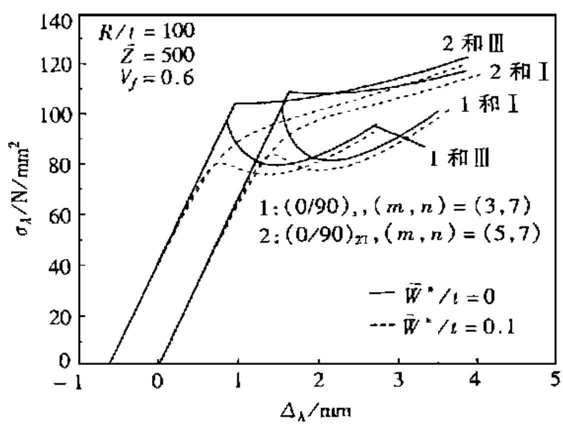

图5 (0/90)s 和(0/90)2T层合圆柱壳在湿热环境下的后屈曲荷载_缩短曲线比较

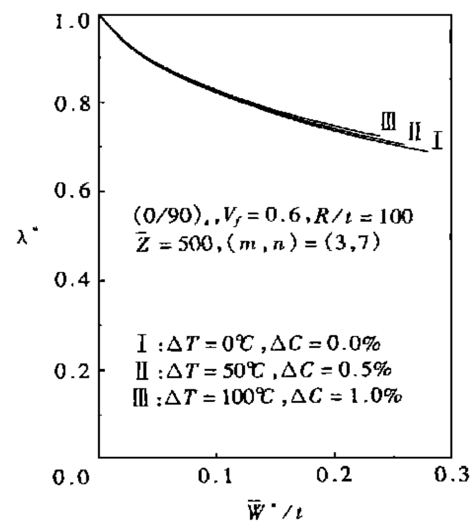

图6 (0/90)s 层合圆柱壳在三种湿热环境条件下的缺陷敏感度曲线比较

图3给出壳体几何参数 Z = (500和200) 对(0/90)s 正交铺设层合圆柱壳后屈曲行为的影响, 湿热环境条件对应Ⅰ 和 Ⅲ• 图示表明, Z = 200的圆柱壳相比 Z = 500的圆柱壳具有较小的端部轴向缩短量•

图4给出不同铺层数 N(= 4和8) 对正交铺设层合圆柱壳后屈曲行为的影响, 湿热环境条

件对应Ⅰ和Ⅲ• 注意到壳板厚度 t 保持不变,因此,随着铺层数增加单层厚度减小• 图示表明,屈曲荷载和后屈曲强度随着铺层数的增加而增加,但 8 层$(0/90)_{2s}$ 圆柱壳屈曲模态为$(m, n) = (4, 7)$,且仅能见到不明显的后屈曲“跳跃”•

图 5 给出$(0/90)_s$ 和$(0/90)_{2T}$正交铺设层合圆柱壳后屈曲荷载_缩短曲线比较,湿热环境条件对应Ⅰ和Ⅲ• 图示表明,$(0/90)_{2T}$层合圆柱壳屈曲模态为$(m, n) = (5, 7)$,且后屈曲平衡路径是稳定的,此时壳结构对初始几何缺陷表现不敏感•

图 6 给出$(0/90)_s$ 正交铺设层合圆柱壳在三种湿热环境条件下的缺陷敏感度曲线,和图 1 结果相对应• 图中 λ^* 等于非完善壳体的极值点荷载除以完善壳体的屈曲荷载(即取 $W^*/t = W/t = 0$)• 图示表明,温度和湿度的增加将减弱壳结构的缺陷敏感度,但本算例仅对应较小的初始几何缺陷•

4　结　　论

为了弄清温度和湿度变化对复合材料层合圆柱薄壳屈曲和后屈曲的影响,发展了一种基于宏_细观力学模型的后屈曲分析方法• 材料性能参数考虑与湿度和温度的变化有关,并以纤维和基体的性能参数和体积比率的显式给出• 壳体屈曲的边界层理论推广用于湿热环境的情况,相应的奇异摄动方法用于确定层合圆柱薄壳的屈曲荷载和后屈曲平衡路径• 给出正交铺设层合圆柱薄壳在湿热环境条件下的参数分析• 计算结果表明,随着温度和湿度变化的增加壳体屈曲和后屈曲强度减小,缺陷敏感度减弱,且温度和湿度的变化,纤维体积比率,壳体几何参数,铺层数,铺层方式和初始几何缺陷材料对层合圆柱薄壳的后屈曲行为有显著影响•

[参　考　文　献]

[1] Birman V, Bert C W. Buckling and post_buckling of composite plates and shells subjected to elevated temperature[J]. ASME J Appl Mech, 1993, **60**(2): 514—519.

[2] SHEN Hui_shen. Post_buckling analysis of imperfect stiffened laminated cylindrical shells under combined external pressure and axial compression[J]. Computers and Structures, 1997, **63**(2): 335—348.

[3] SHEN Hui_shen. Thermal postbuckling analysis of imperfect stiffened laminated cylindrical shells[J], Int J Non_Linear Mech, 1997, **32**(2): 259—275.

[4] SHEN Hui_shen. Thermomechanical postbuckling of stiffened laminated cylindrical shell[J]. ASCE J Engrg Mech, 1997, **123**(5): 433—443.

[5] SHEN Hui_shen. Postbuckling analysis of imperfect stiffened laminated cylindrical shells under combined external pressure and thermal loading[J]. Int J Mech Sci, 1998, **40**(4): 339—355.

[6] SHEN Hui_shen. Thermomechanical postbuckling of composite laminated cylindrical shells with local geometric imperfections[J]. Int J Solids Structures, 1999, **36**(4): 597—617.

[7] Whitney J M, Ashton J E. Effect of environment on the elastic response of layered composite plates [J]. AIAA J, 1971, **9**(9): 1708—1713.

[8] Snead J M, Palazotto A N. Moisture and temperature effects on the instability of cylindrical composite panels[J]. J Aircraft, 1983, **20**(9): 777—783.

[9] Lee S Y, Yen W J. Hygrothermal effects on the stability of a cylindrical composite shell panel[J]. Computers and Structures, 1989, **33**(2): 551—559.

[10] Ram K S S, Sinha P K. Hygrothermal effects on the buckling of laminated composite plates[J].

Composite Structures, 1992, **21**(4): 233—247

[11] Chao L P, Shyu S L. Nonlinear buckling of fiber_reinforced composite plates under hygrothermal effects[J]. J Chinese Institute of Engineers, 1996, **19**(6): 657—667.

[12] Tsai S W, Hahn H T. Introduction to Composite Materials[M]. Westport, CT: Technomic Publishing Co, 1980.

[13] Batdorf S B. A simplified method of elastic stability for thin cylindrical shells[R]. NACA TR_874, 1947.

[14] Bowles D E, Tompkins S S. Prediction of coefficients of thermal expansion for unidirectional composites[J]. J Composite Materials, 1989, **23**(4/6): 370—381.

[15] Adams D F, Miller A K. Hygrothermal microstresses in a unidirectional composte exhibiting inelastic materials behavior[J]. J Composite Materials, 1977, **11**(3): 285—299.

Buckling and Postbuckling of Laminated Thin Cylindrical Shells under Hygrothermal Environments

SHEN Hui_shen

(School of Civil Engineering and Mechanics, Shanghai Jiaotong University, Shanghai 200030, P R China)

Abstract: The influence of hygrothermal effects on the buckling and postbuckling of composite laminated cylindrical shells subjected to axial compression is investigated using a micro_to_macro_mechanical analytical model. The material properties of the composite are affected by the variation of temperature and moisture, and are based on a micromechanical model of a laminate. The governing equations are based on the classical laminated shell theory, and including hygrothermal effects. The nonlinear prebuckling deformations and initial geometric imperfections of the shell were both taken into account. A boundary layer theory of shell buckling was extended to the case of laminated cylindrical shells under hygrothermal environments, and a singular perturbation technique was employed to determine buckling loads and postbuckling equilibrium paths. The numerical illustrations concern the postbuckling behavior of perfect and imperfect, cross_ply laminated cylindrical shells under different sets of environmental conditions. The influences played by temperature rise, the degree of moisture concentration, fiber volume fraction, shell geometric parameter, total number of plies, stacking sequences and initial geometric imperfections are studied.

Key words: structural stability; postbuckling; hygrothermal environments; composite laminated cylindrical shell; a boundary layer theory of shell buckling; singular perturbation technique